Journal of Minerals and Materials Characterization and Engineering, 2025, 13(2), 44-62
https://www.scirp.org/journal/jmmce
ISSN Online: 2327-4085
ISSN Print: 2327-4077

Valorization of Glass Bottles in the Manufacture of Fired Compressed Earth Bricks (CEB)

Talardja Diadi[1], Youssouf Sawadogo[2], Brahima Sorgho[1], Moustapha Sawadogo[1], Mohamed Seynou[1], Lamine Zerbo[1], Philippe Blanchart[3]

[1]UFR-SEA, University Joseph KI-ZERBO, Ouagadougou, Burkina Faso
[2]Tenkodogo University Center, Thomas Sankara University, Ouagadougou, Burkina Faso
[3]CNRS, IRCER, UMR 7315, University of Limoges, Limoges, France
Email: sorghobrahima3@gmail.com

How to cite this paper: Diadi, T., Sawadogo, Y., Sorgho, B., Sawadogo, M., Seynou, M., Zerbo, L. and Blanchart, P. (2025) Valorization of Glass Bottles in the Manufacture of Fired Compressed Earth Bricks (CEB). *Journal of Minerals and Materials Characterization and Engineering*, **13**, 44-62.
https://doi.org/10.4236/jmmce.2025.132004

Received: January 17, 2025
Accepted: March 9, 2025
Published: March 12, 2025

Abstract

The building materials commonly used are energy-intensive, non-ecological, and unsuitable for climatic conditions. For this reason, various research projects have been initiated to develop efficient, appropriate, and accessible building materials. Much of this research focuses on valorizing local materials and available waste. In our study, laterite and bottle glass powder are valorized in the Compressed Earth Bricks (CEB) formulation fired at 750˚C. X-ray fluorescence spectrometry and Attenuated Total Reflectance Fourier Transform Infrared analyzed the chemical composition and chemical bonds. The physicochemical characteristics of the samples, including water absorption and density, were then determined according to standard NF EN 771-1 and ASTM C20-00, respectively. The mechanical analyses of the test pieces were carried out according to standard NF P18-406. Mineralogy of raw materials and the specimens was obtained by X-ray diffraction. Laterite contains significant amounts of 64% kaolinite, 12% hematite, 11% muscovite, 7% goethite, and 5% quartz. Bottle glass powder consists mainly of a glassy phase of amorphous silica and quartz. The 25% glass powder specimens (PV_{25}) had a mechanical strength (11.70 MPa) well over the minimum requirement (4 MPa) for a single plane structure. The thermal performance showed that the 25% amended specimens had a higher thermal conductivity (0.51 $W{\cdot}m^{-1}{\cdot}K^{-1}$) than the control specimens (0.44 $W{\cdot}m^{-1}{\cdot}K^{-1}$). As for the thermal diffusivity, the fired CEB amended by 25% has a better thermal inertia (0.22 mm^2/s compared to 0.33 mm^2/s for the control). 25% amended bricks have been shown to offer superior thermal comfort compared to the controls due to their low thermal diffusivity.

Keywords

Construction, Fired Compressed Earth Bricks (CEB), Laterite, Glass Powder

1. Introduction

Burkina Faso is abundant in a wide variety of clay and laterite raw materials, which are widely utilized in housing construction [1]. However, the sustainability of earth architecture is constrained by various factors (poor mechanical quality and poor water performance) [2]. This has resulted in a shift towards cement construction, a process that is energy-intensive and less environmentally sustainable. In response to these challenges, there have been explorations of alternative approaches aimed at re-establishing the earth as a central element in construction [3] [4]. This approach involves the recycling of agricultural waste in the manufacture of porous bricks, which are lighter than traditional bricks and primarily aimed at enhancing thermal insulation [5]. Indeed, several studies have shown that the mechanical and thermal performance of Compressed Earth Blocks (CEB) can be improved using binders of plant origin. The utilization of natural fibers (e.g., kenaf, bamboo) and agricultural waste (e.g., straw, rice husk, coconut palm) in the manufacture of earth bricks is a further additive [6]-[10]. The incorporation of these additives has been demonstrated to reduce thermal conductivity and diffusivity, thereby enhancing the mechanical properties of the material [9].

The objective of the present study is to explore the development of alternative solutions for the efficient and ecological production of construction materials. The recycling of glass bottle waste would be a promising alternative [11]. This particular waste is both accessible and inexpensive, and it has a low melting point. Indeed, glass occupies a privileged place within the food industry sector due to its safety [12]. However, there is a paucity of research focusing on glass bottles as additives in the production of bricks. The recovery of glass bottle waste emerges as a promising alternative, offering significant environmental and economic benefits. From an environmental perspective, this approach prevents the release of glass into landfills, contributing to the reduction of waste disposal costs and the mitigation of environmental impacts. From an economic perspective, the utilization of glass bottle waste as an additive in the production of CEBs can result in a substantial reduction in production costs, enhancing the economic viability and sustainability of the manufacturing process [13]. The present study is concerned with the analysis of the physicochemical and mineralogical properties of laterite and glass bottle powder to evaluate their potential application in the formulation of construction earth materials. The physico-mechanical and thermal properties of the developed specimens are also evaluated to validate their use in the construction field.

2. Raw Materials

The present study focused on two raw materials: laterite, a basic raw material, referenced as HOUN, and crushed glass bottles, pulverized into powder, referenced as PV. The laterite, designated as HOUN, was sourced from a lateritic site in the locality of Houndé (**Figures 1(a)-(b)**), situated in the Tuy province of the Hauts-Bassins region in the western part of Burkina Faso. The precise geographical

location of the site is specified by its geographic coordinates: 3˚31'49" West Longitude and 11˚30'32" North Latitude. The local population exploits the HOUN sample site for the manufacture of local construction materials.

PV sample, an additive raw material, was obtained from glass bottles of local juice. These bottles are not recycled and are disposed of in the environment after use (**Figure 2(a)**). Following collection from designated refreshment stands, the bottles undergo a series of processing steps that include washing, drying, crushing, and sieving to yield a powder with a particle size of less than 250 µm (**Figures 2(b)-(c)**).

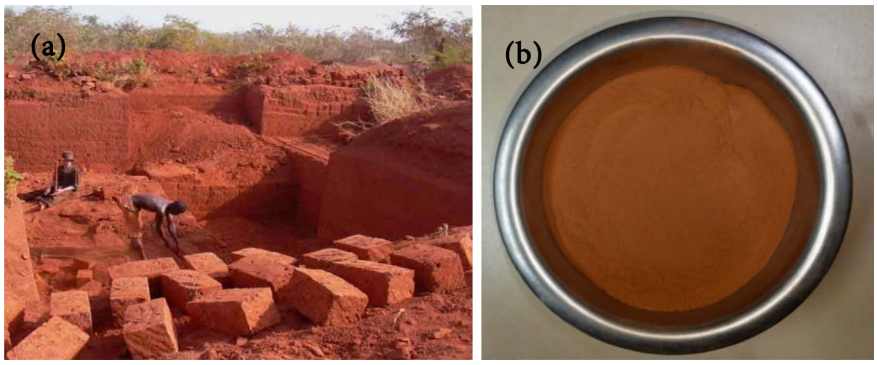

Figure 1. (a) HOUN mining site; (b) Crushed HOUN sample.

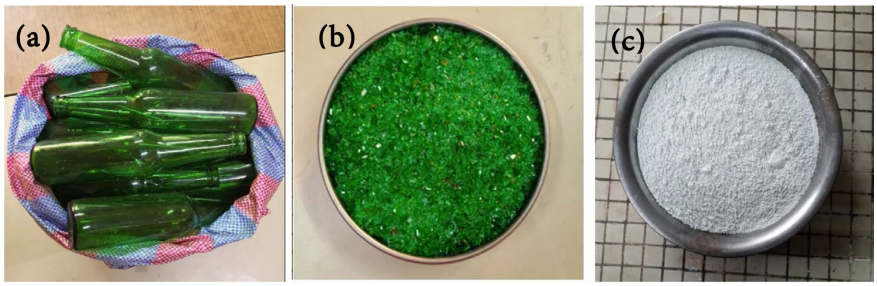

Figure 2. (a) Collected glass bottles; (b) Crushed glass bottles; (c) PV sample.

3. Methods

3.1. Characterization Techniques

Atterberg limits are frequently utilized to characterize clays. The liquid limit is defined as the water content of a material when it transitions from a liquid to a plastic state, while the plastic limit signifies the water content when it shifts from a solid to a plastic state. The plasticity index, defined as the difference between these two limits, is influenced by the nature of the clay minerals. The measurements are carried out by the NF P 94-051 standard [14], which involves wet sieving of the laterite, followed by the preparation of a paste to determine the two limits using a Casagrande cup and paste rods.

The chemical composition of the raw materials was determined with X-ray fluorescence. The raw material powders were characterized by X-ray diffraction (XRD). The instrument utilized in this study is a Philips PW 1729 diffractometer,

which operates at 40 kV and 40 mA with CuKα radiation. The semi-quantitative composition of the mineral phases of the samples was evaluated using relation (1) proposed by de Yvon *et al.* (1982) [15], which is as follows:

$$T(a) = \sum Mi\, Pi(a) \tag{1}$$

- $T(a)$: content (%) of chemical element "a";
- Mi: content (%) of mineral "i" in the material studied and containing element "i";
- $Pi(a)$: proportion of element "a" in mineral "i".

The density of the test pieces was evaluated by the NF EN 771-1 (2004) standard [16]. The test pieces, previously dried at 105˚C and baked at 750˚C, were weighed in air, then covered with paraffin and weighed again in air. They were then weighed after being immersed in water.

The determination of water absorption was carried out by the ASTM C20-00 standard (2010) [17]. The mass of the test piece that has undergone the cooking process at 750˚C in an oven is determined. The test piece is then subjected to an immersion in boiling water for two hours. Following this, the test pieces are removed from the water and allowed to cool for four hours. Thereafter, they are removed from the water, and the mass of the wet state, designated m_a, is determined. The percentage of water absorption (A) for each test piece is expressed by the following relation (2) [17]:

$$A(\%) = \frac{m_a - m_s}{m_s} \times 100 \tag{2}$$

m_s: dry mass of the test piece; m_a: wet mass of the test piece.

The compressive strength of CEBs is defined as the maximum stress that the material can support before failure. The specimen is subjected to a monotonically increasing load until rupture. The compressive strength is defined as the ratio between the maximum load at failure and the cross-sectional area of the specimen. The compressive strength of CEBs is determined by relation (3). The experimental procedure is conducted using the established protocol outlined in NF P18-406 [18].

$$R_c = \frac{10F}{S} \tag{3}$$

R_c: compressive strength of the specimen (MPa); F: maximum load supported by the specimen (kN); and S: average value of the section (cm^2).

In addition to mechanical resistance, the thermal performance of CEBs is a critical factor in ensuring the indoor comfort of a building. The measurements are conducted using an SH-1 probe (with a diameter of 1.3 millimeters, a length of 3 centimeters, and an operating range of 0.02 to 2 $W{\cdot}m^{-1}{\cdot}K^{-1}$ with an accuracy of ±10%) connected to a KD2 Pro thermal properties analyzer [9]. The probe is inserted into two apertures made in the center of one of the faces of the CEB, previously dried so that there is no contact with air (**Figure 3**).

3.2. Procedure for Shaping Test Pieces

Cylindrical test pieces with a diameter of 5 cm and a height of 10 cm are produced

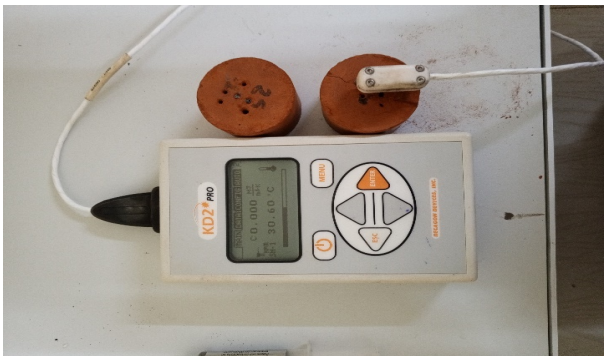

Figure 3. Image of the KD2 Pro device.

for the various tests from two raw materials: laterite identified as HOUN and bottle glass powder. The production of CEBs commences with the grinding of the HOUN and PV samples until a particle size of less than 250 µm for HOUN and 106 µm for PV is obtained, respectively. Studies by Turco, C. *et al.* (2024) show that CEBs with finer particles exhibit poorer heat conduction and heat diffusion [19]. The glass must have a particle size below the limit of the pan mills used in brickmaking (<1 mm) [20]. The grinding is carried out using a CERADEL brand ball mill. The powder obtained after grinding is then placed in an oven at 105˚C for twenty-four (24) hours before mixing. Subsequently, a series of mixtures are meticulously prepared and subsequently dried and homogenized. Previous studies have used glass powder as a stabilizing additive (CEB). This is the case, for example, of Izemmouren Ouarda (2016), who used up to 40% of the contents of glass powder with lime in the formulation of CEB [21]. Serwan Kh. Rafiq (2022) studies the impact of glass waste on the flexural, compressive, and direct tension bonding strengths of Masonry bricks. These bricks have been modified with green waste glass using 5%, 10%, and 15% as a partial replacement of fine aggregate in a mortar [22]. We have been inspired by this previous research work in the choice of the composition of our CEBs in terms of the percentage of glass powder. To meet the objective of the study, five series of fired CEBs were produced by varying the percentage of PV (0, 20%, 25%, 30%, and 35%) of the weight of the dry mixture. The composition of the mixtures is given in **Table 1**. Conventionally, CEB materials are composed of clay (60% to 95%), sand (0 to 40%), and a mineral or organic stabilizer (0 to 40%) [21]-[23]. The total mass of the mixture is 900 g. For each mixture, a varying amount of water (water mass ≤ 10% of the total mass of the mixture) is added until a slightly damp mixture is obtained. The manual mixing process is conducted for a duration of 10 to 15 minutes to disintegrate the clumpy clay and ensure thorough integration of the components. To facilitate the maturation process, the resultant pastes were stored in hermetically sealed containers within an ambient temperature room for 48 hours. Following this, the moistened pastes of constant mass (150 g of the moistened mixture) are introduced into a cylindrical mold (50 × 160) mm^2 and then pressed. The test pieces were then unmolded on site and dried in the shade for 21 days at room temperature. The pressing was accomplished through the utilization of a Magnolfi-Bigali-

type hydraulic press, which employed compression to ensure the desired density was achieved. The diagrammatic representation of the compressed earth brick production process is illustrated in Figure 4.

Table 1. Composition of the nuances of the test pieces.

Sample references	PV_0	PV_{20}	PV_{25}	PV_{30}	PV_{35}
% PV	0	20	25	30	35
PV weight (g)	0	180	225	270	315
HOUN weight (g)	900	720	675	630	585
Water weight (g)	90	85.5	81	76.5	72

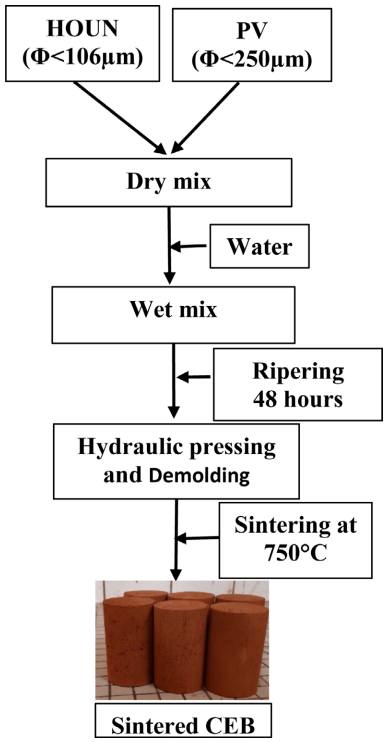

Figure 4. Simplified diagram of the brick-making process.

Following the process of demolding, the specimens were subjected to a drying period at ambient temperature. Thereafter, they were baked at a temperature of 105˚C for 24 hours to remove the water of hydration. Throughout the drying process, it is imperative to exercise meticulous control over the duration, temperature, and humidity. Failure to do so may result in the bricks bursting or cracking due to the expansion of steam within the mass. After this, the specimens underwent a cooling phase, after which they were subjected to a heat treatment at a temperature of 750˚C for two hours in a Nabertherm oven, specifically the MORE THAN HEAR P300 model, with a heating rate of 5˚C per minute (**Figures 5(a)-(b)**). This process was conducted with the aid of a heating rate controller. The calcination temperature was set at 750°C for two primary reasons:

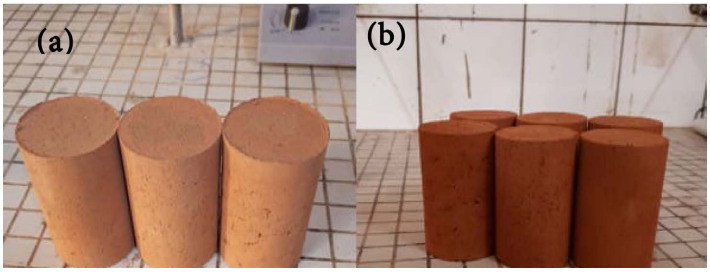

Figure 5. (a) Test tubes before sintering; (b) Test tubes after sintering

1) To obtain terracotta products at low temperatures;

2) To reach the softening interval of the glass powder, which is around 700˚C [24].

The firing temperature is chosen to melt a significant amount of glass powder without altering the physical state of the clays.

The different formulated specimens will then be characterized to evaluate their loss of mass on fire, density or water absorption, thermal conductivity, and mechanical resistance.

4. Results

4.1. Chemical Characterization of Raw Materials

As illustrated in **Table 2**, the chemical composition of the HOUN sample is as follows: The major oxides present in this sample are alumina (29.71%), silica (39.52%), and iron oxide (18.23%) [25]. The SiO_2/Al_2O_3 ratio of 1.33 indicates the presence of free silica (quartz) in the sample, as this value is greater than 1.18 for pure kaolinite [26]. The presence of iron oxide (18.23%) is responsible for the red-yellow coloration of the sample. The oxides CaO, MgO, Na_2O, and K_2O are present in low concentrations. It is noteworthy that the alkaline oxides (Na_2O and K_2O) function as flux, thereby influencing the sanding reactions and the formation of the vitreous phase during the heat treatment process. These reactions are pivotal in determining the final properties of the brick. PV sample is composed of the following chemicals: It is evident from this table that the predominant oxide is silica (SiO_2). In addition, sodium oxide (Na_2O), lime (CaO), magnesium oxide (MgO), and alumina (Al_2O_3) are present in significant proportions. Some of these elements are present in very small quantities and play a role either in stabilizing the amorphous structure of the glass or in coloring (the visual aspect of the glass). The presence of lime (CaO) is indicative of the potential for PV to undergo pozzolanic activity in HOUN, thereby yielding resilient materials. The content of alkali oxide (K_2O and Na_2O), which constitutes the fluxing phases in PV, is 13.3%

Table 2. Chemical composition of HOUN and PV (%).

Sample	Al_2O_3	SiO_2	Fe_2O_3	CaO	MgO	Na_2O	K_2O	Others	Total
HOUN	29.71	39.52	18.23	0.03	0.05	0.12	1.32	11.02	100.00
PV	1.50	72.50	0.10	9.30	3.00	13.00	0.30	0.30	100.00

[27]. These oxides contribute to reducing the melting temperature of the minerals by promoting the dissolution of free silica and the formation of glassy phases. However, it is notable that the presence of iron oxide (0.10%) is comparatively low, in contrast to the bibliographic data, which typically ranges from 4.08% [28] [29]. These results remain compatible with the chemical composition of classic soda-lime glass [30] [31].

4.2. Geotechnical Characterization of Raw Materials

The Atterberg limits were evaluated and recorded in **Table 3**. These values were then compared with the recommended values According to CRATerre-EAG [32] for the development of CEBs. The values of the liquid limit (WL), the plastic limit (WP), and the plasticity index (PI) of HOUN, respectively 30.48%, 23.20%, and 7.28%, are included in the ranges of the materials used for CEBs (WL = 25% to 50%; WP = 10% to 25%; PI = 7% to 29%). Notably, only the WL (30.48%) and the PI (7.28%) are included in the zone of preferred materials for CEBs (WL = 30% to 35%; PI = 7% to 18%). The WP (23.20%) is marginally outside the WP range of preferred materials (WP = 12% to 22%). The excellent geotechnical workability of the samples used is demonstrated by the measured Atterberg limits. Materials are only considered to be easily mouldable if their IP index is ≤20 and their liquid limit is 15% ≤ wL ≤ 35% [33]. The results obtained allow us to confirm that our sample shows a plasticity fully adapted to producing CEB [34].

Table 3. HOUN Atterberg limits and area delimiting the Atterberg limits for CEBs [32].

Atterberg limits	HOUN	Limit zone for a CEB	Preferential zone for a CEB
Liquid limit W_L (%)	30.48	25 to 50	30 to 35
Plastic W_P (%)	23.20	10 to 25	12 to 22
Plasticity index I_p (%)	7.28	7 to 29	7 to 18

4.3. Mineralogy Characterization of Raw Materials

The infrared spectrum (**Figure 6(a)**) of HOUN exhibits three distinct spectral regions [1]. The first region is between 3650 and 3400 cm^{-1}, the second between 1650 and 900 cm^{-1}, and the third between 800 and 400 cm^{-1}. The spectrum displays specific bands of particular significance, including vibration bands at 3695 and 3618 cm^{-1}, 1111 and 694 cm^{-1}, 795 cm^{-1}, and 1086 cm^{-1}. These absorption bands are linked to specific vibrations of the bonds, including Al-OH, Si-O, Si-O-Si, and Fe-OH [35]-[37]. These vibration bands indicate the occurrence of specific phases, including kaolinite and/or muscovite, quartz, goethite, and/or hematite [38].

The PV spectrum (**Figure 6(b)**) shows two primary characteristic bands associated with bond vibrations. These bands correspond to Si-O and Si-O-Si bonds, suggesting that quartz is the predominant phase in the sample [24] [39]-[41].

As demonstrated in **Figure 7(a)**, the diffractogram indicates that the crystallized phases of the HOUN sample are primarily kaolinite, quartz, goethite, muscovite,

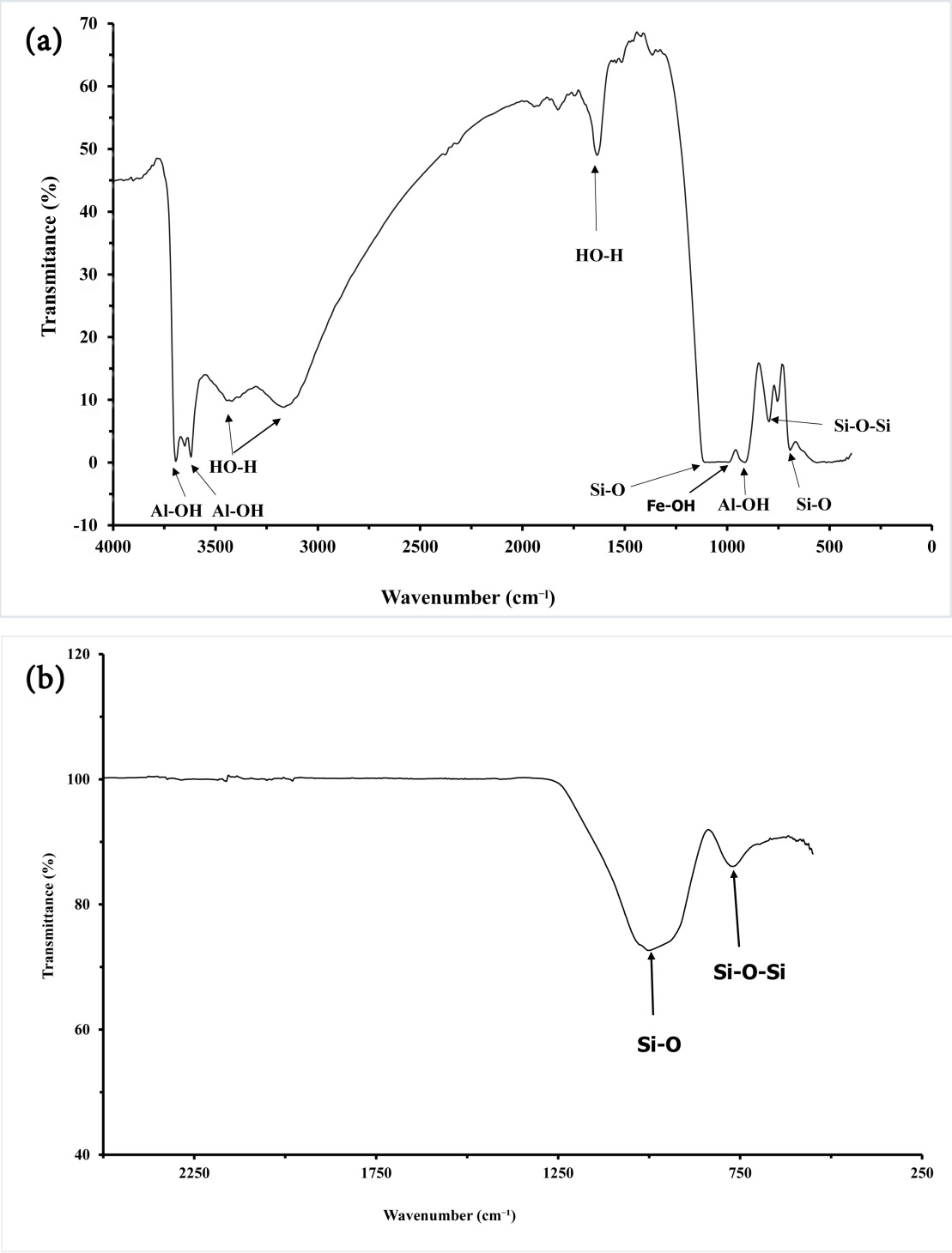

Figure 6. (a) IR spectrum of HOUN; (b) IR spectrum of PV.

and hematite. Consequently, it can be deduced that the composition of HOUN is a mixture of plasticizer (kaolinite and muscovite), dye (goethite and hematite), and degreaser (quartz). The composition of HOUN renders it well-suited for utilization in the manufacture of adobes and CEBs, with the plasticizers serving the function of a matrix and the degreasers acting as reinforcements.

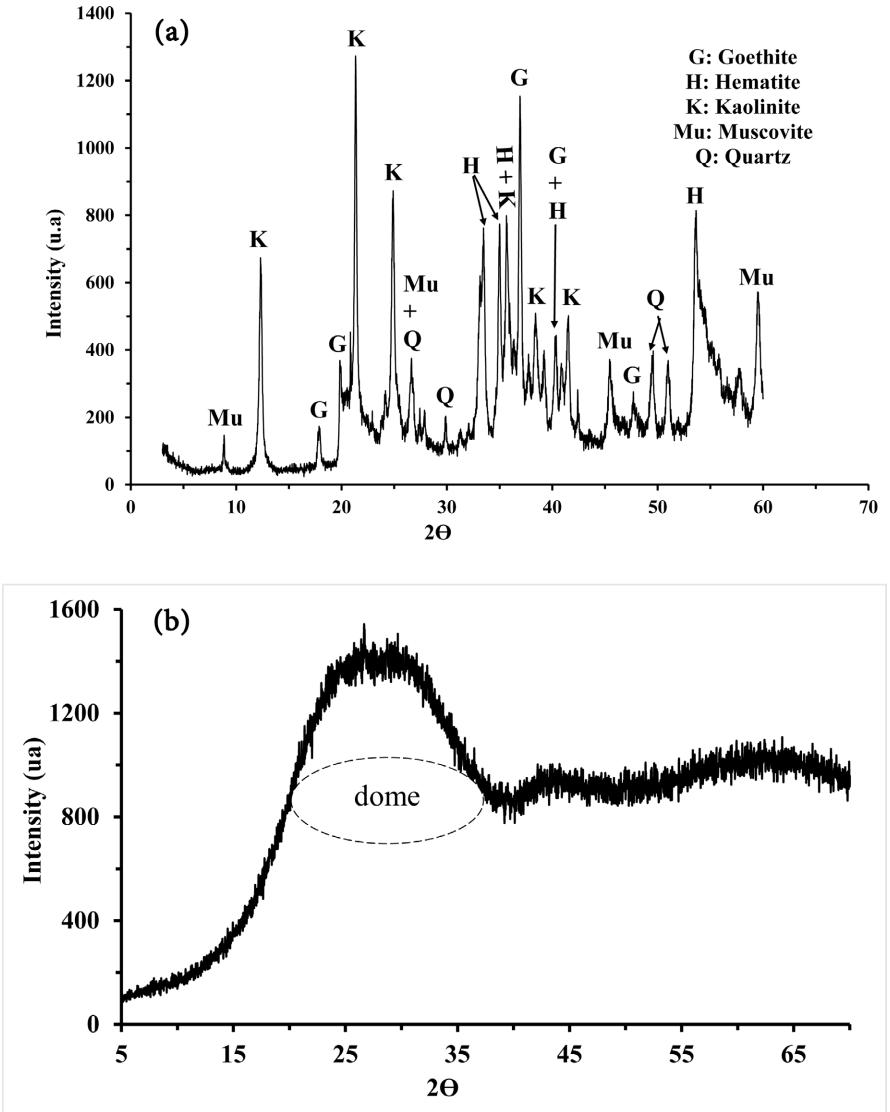

Figure 7. (a) HOUN diffractogram; (b) PV diffractogram

The results of the semi-quantitative analysis (Table 4) demonstrate that HOUN contains the following phases: 64% kaolinite, 12% hematite, 11% muscovite, 7% goethite, and 5% quartz. The predominant mineral phase is kaolinite. The presence of quartz indicates the potential for free silica, as evidenced by the SiO_2/Al_2O_3 ratio. The relatively high contents of hematite and goethite (12% + 7% = 19%) suggest a potential role for these minerals as colorants in HOUN.

Table 4. Semi-quantitative analysis results of HOUN.

Phases	Kaolinite	Muscovite	Quartz	Hematite	Goethite	Total
%	64	11	5	12	7	99

The analysis of the PV diffractogram (Figure 7(b)) demonstrated that the material is entirely amorphous, a conclusion that is substantiated by the presence of

a broad hump between 20˚ and 40˚ (2θ) and the presence of background noise on the DRX curve. These DRX results confirm that the silica contained in PV is amorphous (glassy phase) [29] [42] [43]. No crystallization peak is visible on the diffractogram. The low melting point of the studied PV (approximately 700˚C), in conjunction with the presence of lime in its composition, indicates its potential application as an adjuvant in the manufacture of fired compressed earth bricks (CEB).

4.4. Physicochemical, Thermal, and Mechanical Characterizations of Formulated Test Specimens

The characteristics of the specimens evaluated are apparent density, water absorption, compressive strength, conductivity, and thermal diffusivity.

The bulk density of clay bricks increased with an increase in the amount of waste glass. As a result, the bulk densities of bricks containing waste glass were in the range of 1.72 and 1.76. These results are in line with those that have been found by other researchers [29] [42]. The density curve (**Figure 8**) demonstrates a downward trend. The substitution of HOUN (density 2.72) for less dense PV (density 2.50) is substantiated by the reduction in specimen density [31].

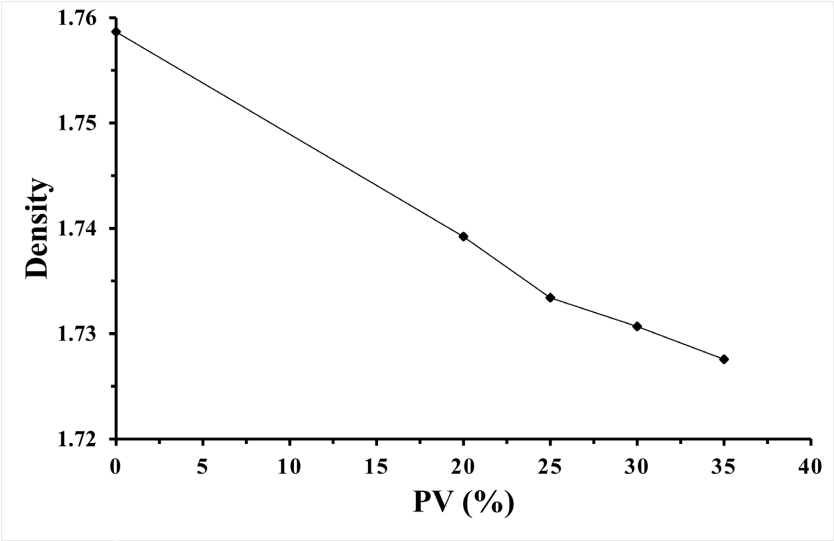

Figure 8. Density of test specimens.

The variation in the percentage of water absorption as a function of the percentage of PV is illustrated in **Figure 9**. It is evident from this figure that the water absorption decreases with an increase in the amount of glass powder in the test pieces. This phenomenon can be attributed to the melting of the glass, which occurs at higher temperatures, leading to the closure of the pores within the test pieces. Consequently, it can be posited that the incorporation of glass powder into the formulated material results in the closure of pores when the material is subjected to the glass melting temperature, thereby leading to the observed low water absorption [44].

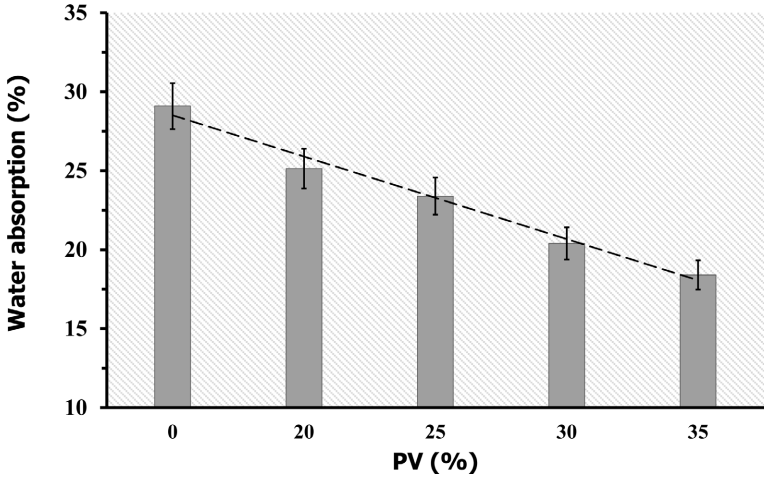

Figure 9. Water absorption of test tubes.

Figure 10 demonstrates the variances in the compressive strength of the specimens as a function of the percentage of glass powder. The specimens exhibit remarkably high mechanical strengths. The incorporation of glass into the laterite has been demonstrated to enhance the compressive strength of the bricks. The maximum compressive strength (11.70 MPa) is observed in specimens containing 25% glass powder, in comparison to 7.94 MPa in the control specimens. This enhancement in strength can be rationalized by the favorable cohesion between the clay phase and the glass powder, as well as the firing temperature, which fosters the consolidation of the specimens. However, beyond 25% glass powder, a decrease in strength is observed, which can be attributed to an excess of glass powder in the material, thereby hindering effective interaction between the glass powder and the granular skeleton.

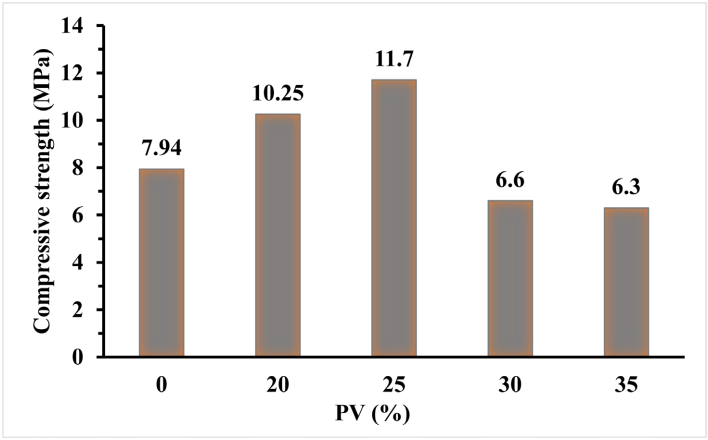

Figure 10. Mechanical resistance of the specimens as a function of the PV rate.

Thermal conductivity and diffusivity were evaluated, with the specimens exhibiting superior mechanical resistance and the control specimen. The results of the analysis indicate that the specimens amended with 25% glass powder exhibit a thermal conductivity of 0.51 $W \cdot m^{-1} \cdot K^{-1}$ and a diffusivity of 0.22 mm^2/s. In contrast,

the control specimens exhibited thermal conductivity of 0.44 $W \cdot m^{-1} \cdot K^{-1}$ and thermal diffusivity of 0.33 mm^2/s.

5. Discussion

Alumina and silica (**Table 2**) are the predominant components of the HOUN sample and are also the primary constituents of clay bricks. When these oxides are mixed with water in adequate proportions, they facilitate the shaping of bricks and contribute to limiting exclusive shrinkage, thus reducing the risk of cracking [45]. The substantial iron oxide content of the mixture is responsible for the pigmentation of the formulated bricks. The presence of goethite and hematite has been demonstrated to have a significant impact on the firing temperature. However, it should be noted that their effect on shrinkage during the cooling process can have deleterious consequences on the materials [46]. Alkaline oxides, such as sodium (Na_2O) and potassium (K_2O) oxides, act as fluxes by contributing to the reactions of sanding and the formation of the vitreous phase. These reactions are responsible for the final properties of the brick. The presence of lime (CaO) in HOUN has been shown to induce pozzolanic reactions with the amorphous phase of PV, thereby enhancing the material's resistance [28]. The findings underscore the potential for the utilization of glass bottle waste and laterite in construction applications. Consequently, a combination of laterite and glass bottle powder was utilized in the fabrication of compressed earth bricks (CEB), which were subjected to firing at a moderate temperature of 750˚C.

Increasing the firing temperature up to 750˚C has been shown to result in the presence of a slightly more abundant vitreous phase in the test pieces. This phase has been demonstrated to contribute to the reduction of the pores contained within the material, thereby causing the water absorption rate to fall [47]. As demonstrated in **Figure 9**, the water absorption rate of the control samples exceeds the stipulated requirements of the SNI 15-2094-2000 standard [48] (20%), with the majority of samples falling within this range. The density of CEB typically ranges from 1.5 g/cm^3 to 2 g/cm^3. According to previous studies, the density of CEB is contingent on the pressure applied during compaction, the nature of the soil, and the nature of the additive (Omar *et al.*, Stabilization of CEB by cement, 2023). In the study by Omar *et al.*, the density of CEB ranged from 1.607 g/cm^3 to 1.90 g/cm^3 [49].

The compressive strength of the bricks increased, reaching a maximum value of 11.7 MPa, or 67.86%, compared to the control. This enhancement can be ascribed to the robust bonds formed between the laterite particles and the glass in conjunction with the firing temperature. This observed compressive strength value is commensurate with the range of 12.5 to 40 MPa, which are considered to be the requisite values for fired clay bricks [50]. The compressive strength of the bricks demonstrates satisfactory performance for application in building (**Figure 11**).

The incorporation of 25% glass in the specimens resulted in a 15.9% increase in thermal conductivity. This phenomenon can be attributed to the presence of

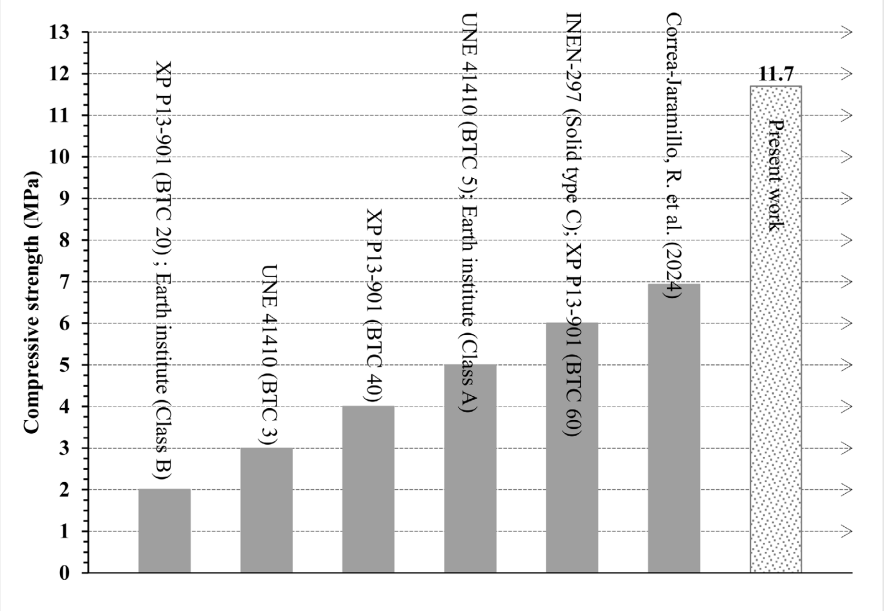

Figure 11. Compressive strength results [51] [52].

molten glass within the material, thereby resulting in the formation of a non-porous structure. This results in a reduction of thermal insulation due to the increased conductivity, facilitating greater heat penetration into the material. The variation in conductivity is undoubtedly related to a variation in the porosity of the material, the intrinsic composition of each sample, and the cohesion of the material [53]. The increase in firing temperature increased firing shrinkage combined with a decrease in water absorption. As a result, a denser brick was formed, and the thermal conductivity was consequently increased [54]. The conductivity values are low enough to conclude that the contribution of PV while improving the physical and mechanical properties, does not alter the thermal properties. This is a clear advantage for these materials. The low thermal diffusivity exhibited by specimens containing 25% glass indicates a prolonged thermal phase shift, consequently resulting in reduced thermal inertia. The ensuing analysis will be classified according to the designated performance classes outlined in the Earth Construction Treaty (1989) to facilitate the dissemination of results and the facilitation of future discourse [55]. The classification is delineated in **Table 5**. According to this classification, the PV_{25} specimens formulated from 25% PV and 75% HOUN are part of class B with a thermal conductivity of 0.51 $W{\cdot}m^{-1}{\cdot}K^{-1}$. The estimated thermal characteristics fall within the intervals reported in the literature. Thermal conductivity values stabilized CEBs generally range between 0.40 and 1.20 $W{\cdot}m^{-1}{\cdot}K^{-1}$ and thermal diffusivity between 3.02×10^{-7} and 4.82×10^{-7} $m^2{\cdot}s^{-1}$ [19]. The CEBs formulated will, therefore, contribute to the natural air conditioning of buildings, to their hygrometric balances, and to electricity savings.

The study's findings demonstrate that specimens fortified with 25% glass exhibit thermal conductivity and diffusivity values analogous to those of adobe, ranging from 0.46 to 0.81 $W{\cdot}m^{-1}{\cdot}K^{-1}$. This observation substantiates their suitability

Table 5. Class of thermal performance of earth construction (1989) [55].

Class	A	B	C	D
Thermal conductivity (W/m/K)	0.23 to 0.46	0.46 to 0.81	0.81 to 0.93	0.93 to 1.04

for incorporation into construction applications, thereby ensuring their practical relevance. Consequently, the amended materials' heat propagation time is longer than the control samples. Consequently, it can be concluded that the materials containing 25% glass will provide superior thermal insulation properties in comparison to the control materials.

6. Conclusion

The present study constitutes an investigation into the utilization of laterite in the fabrication of compressed earth bricks (CEB), subjected to a firing temperature of 750˚C, in conjunction with the incorporation of glass bottle powder as an additive. The coupling of several analysis techniques characterized the raw materials. The analysis results indicated that the laterite is composed of a significant clay phase (kaolinite and muscovite) associated with non-clay phases (quartz, goethite, and hematite). The glass powder is primarily composed of quartz in the form of an amorphous phase. The specimens produced were then subjected to a series of physicochemical, mineralogical, and thermal tests. The findings of these assessments revealed a substantial decline in apparent density and water absorption, concomitant with an augmentation in the proportion of glass powder within the specimens. Furthermore, the mechanical resistance values of the different fired specimens (CEB) were found to exceed the minimum requirement of 4 MPa for a single-level construction. The specimens containing 20% and 25% glass powder have the highest mechanical strengths of 10.25 and 11.70 MPa, respectively. The significant results obtained in the mechanical and durability tests demonstrate the beneficial effect of these glass powder additions in improving mechanical resistance and durability. However, a study of the effect of the dosage of additions overtime on the mechanical resistance and durability of fired CEBs is necessary to confirm their long-term influences. The thermal performances evaluated on the control specimens and those amended at 25% indicate that the bricks amended at 25% have superior thermal comfort compared to the controls because of their low thermal diffusivity. However, further research is required to study the erosion behavior and the behavior against chemical attacks and fire of our formulated bricks to confirm their use in construction.

Acknowledgements

The authors thank the editors and anonymous reviewers for their helpful comments and suggestions.

Conflicts of Interest

The authors declare no conflicts of interest regarding the publication of this paper.

References

[1] Ouedraogo, R.D., Bakouan, C., Sorgho, B., Guel, B. and Bonou, L.D. (2020) Caractérisation d'une latérite naturelle du Burkina Faso en vue de l'élimination de l'arsenic (III) et l'arsenic (V) dans les eaux souterraines. *International Journal of Biological and Chemical Sciences*, **13**, 2959-2977. https://doi.org/10.4314/ijbcs.v13i6.41

[2] Sanou, I. (2019) Mineralogy, Physical and Mechanical Properties of Adobes Stabilized with Cement and Rice Husk Ash. *Science Journal of Chemistry*, **7**, 1-10. https://doi.org/10.11648/j.sjc.20190701.11

[3] Zhang, Z., Wong, Y.C., Arulrajah, A. and Horpibulsuk, S. (2018) A Review of Studies on Bricks Using Alternative Materials and Approaches. *Construction and Building Materials*, **188**, 1101-1118. https://doi.org/10.1016/j.conbuildmat.2018.08.152

[4] Nshimiyimana, P., Fagel, N., Messan, A., Wetshondo, D.O. and Courard, L. (2020) Physico-Chemical and Mineralogical Characterization of Clay Materials Suitable for Production of Stabilized Compressed Earth Blocks. *Construction and Building Materials*, **241**, Article ID: 118097. https://doi.org/10.1016/j.conbuildmat.2020.118097

[5] Zhang, L. (2013) Production of Bricks from Waste Materials—A Review. *Construction and Building Materials*, **47**, 643-655. https://doi.org/10.1016/j.conbuildmat.2013.05.043

[6] Millogo, Y., Aubert, J., Hamard, E. and Morel, J. (2015) How Properties of Kenaf Fibers from Burkina Faso Contribute to the Reinforcement of Earth Blocks. *Materials*, **8**, 2332-2345. https://doi.org/10.3390/ma8052332

[7] Abessolo, D., Biwole, A.B., Fokwa, D., Ganou Koungang, B.M. and Yebga, B.N. (2020) Effets de la Longueur et de la Teneur des Fibres de Bambou sur les Propriétés Physicomécaniques et Hygroscopiques des Blocs de Terre Comprimée (BTC) Utilisés dans la Construction. *Afrique Science*, **16**, 13-22.

[8] Djadouf, S., Tahakourt, A., Chelouah, N. and Merabet, D. (2011) Étude de l'Influence des Ajouts (Grignon d'Olive et Foin) sur les Caractéristiques Physico-Mécaniques de la Brique de Terre Cuite. *Communication Science & Technologie*, **9**, 1-7.

[9] Sory, N., Ouedraogo, M., Messan, A., Sanou, I., Sawadogo, M., Jeremy Ouedraogo, K., *et al.* (2022) Mechanical, Thermal and Hydric Behavior of the Bio-Sourced Compressed Earth Block (B-CEB) Added to Peanut Shells Powder. *Advances in Materials*, **11**, 1-13. https://doi.org/10.11648/j.am.20221101.11

[10] Bobet, O., Nassio, S., Seynou, M., Remy, B., Zerbo, L., Sanou, I., *et al.* (2020) Characterization of Peanut Shells for Their Valorization in Earth Brick. *Journal of Minerals and Materials Characterization and Engineering*, **8**, 301-315. https://doi.org/10.4236/jmmce.2020.84018

[11] Milohin, G.S.G. (2019) Valorisation de Rebuts de Bouteilles en Verre et des Cendres de Bois dans la Fabrication de Briques en Argile Cuite. Master's Thesis, Université d'Abomey-Calavi (Bénin).

[12] Verghese, K., Lewis, H., Lockrey, S. and Williams, H. (2013) The Role of Packaging in Minimising Food Waste in the Supply Chain of the Future. *Technical Report*, **3**, 1-49. https://doi.org/10.13140/2.1.4188.5443

[13] Xin, Y., Robert, D., Mohajerani, A., Tran, P. and Pramanik, B.K. (2023) Transformation of Waste-Contaminated Glass Dust in Sustainable Fired Clay Bricks. *Case Studies in Construction Materials*, **18**, e01717. https://doi.org/10.1016/j.cscm.2022.e01717

[14] Association Française de Normalisation (AFNOR) (1993) Sols Reconaissance et Essais-

Détermination des Limites d'Atterberg. Limite de Liquidité à la Coupelle-Limite-de Plasticité au Rouleau. NF P 94-051.

[15] Yvon, J., Liétard, O., Cases, J. and Delon, J. (1982) Minéralogie des argiles kaoliniques des Charentes. *Bulletin de Minéralogie*, **105**, 431-437. https://doi.org/10.3406/bulmi.1982.7565

[16] Association Française de Normalisation (AFNOR) (2004) Spécifica-tions pour éléments de maçonnerie Partie1: Briques de terre cuite. NF EN 771-1.

[17] ASTM C20-00 (2010) Standard Test Methods for Apparent Porosity, Water Absorption, Apparent Specific Gravity, and Bulk Density of Burned Refractory Brick and Shapes by Boiling Water.

[18] Association Française de Normalisation (1981) Essai de Compression des Eprouvettes en Béton Durci. AFNOR. NF P 18-406.

[19] Turco, C., Paula Junior, A., Jacinto, C., Fernandes, J., Teixeira, E. and Mateus, R. (2024) Influence of Particle Size on Compressed Earth Blocks Properties and Strategies for Enhanced Performance. *Applied Sciences*, **14**, Article 1779. https://doi.org/10.3390/app14051779

[20] Dondi, M., Guarini, G., Raimondo, M. and Zanelli, C. (2009) Recycling PC and TV Waste Glass in Clay Bricks and Roof Tiles. *Waste Management*, **29**, 1945-1951. https://doi.org/10.1016/j.wasman.2008.12.003

[21] Izemmouren, O. (2016) Effet des Ajouts Minéraux sur la Durabilité des Briques de Terre Comprimée. Master's Thesis, Université Mohamed Khider-Biskra.

[22] Rafiq, S.K. (2022) Impact of Glass Waste on the Flexural, Compressive, and Direct Tension Bonding Strengths of Masonry Bricks. *Journal of Engineering*, **28**, 85-106. https://doi.org/10.31026/j.eng.2022.11.07

[23] Fiche Technique (2021) Bloc stabilisé BTCs Cycle Terre. 191210.

[24] Le Losq, C., Tarrago, M., Blanc, W., Georges, P., Hennet, L., Zanghi, D., *et al.* (2022) Méthodes d'analyse des verres. *Matériaux & Techniques*, **110**, Article No. 403. https://doi.org/10.1051/mattech/2022041

[25] Sory, D., Sanou, Y., Kaboré, R. and Paré, S. (2024) Efficiency of Two Laterites in Cyanide Removal from Aqueous Solutions: Equilibrium and Kinetic Studies. *Science Journal of Analytical Chemistry*, **12**, 38-45. https://doi.org/10.11648/j.sjac.20241203.12

[26] Ouattara, S., Sorgho, B., Sawadogo, M., Sawadogo, Y., Seynou, M., Blanchart, P., *et al.* (2021) Development and Characterization of Geopolymers Based on a Kaolinitic Clay. *Science Journal of Chemistry*, **9**, 160-170. https://doi.org/10.11648/j.sjc.20210906.15

[27] Sawadogo, Y., Zerbo, L., Sawadogo, M., Seynou, M., Gomina, M. and Blanchart, P. (2020) Characterization and Use of Raw Materials from Burkina Faso in Porcelain Formulations. *Results in Materials*, **6**, Article ID: 100085. https://doi.org/10.1016/j.rinma.2020.100085

[28] Behim, M. and Ali Boucetta, T. (2013) Valorisation du verre à bouteille comme addition fine dans les bétons autoplaçants. *Environnement, Ingénierie & Développement*, **65**, 20-28. https://doi.org/10.4267/dechets-sciences-techniques.932

[29] Phonphuak, N., Kanyakam, S. and Chindaprasirt, P. (2016) Utilization of Waste Glass to Enhance Physical-Mechanical Properties of Fired Clay Brick. *Journal of Cleaner Production*, **112**, 3057-3062. https://doi.org/10.1016/j.jclepro.2015.10.084

[30] Bouchikhi, A. (2020) Optimisation de la Valorisation des Déchets de Verre et de Sédiments dans des Liants Recomposés: Activation—Formulation de Mortiers—Stabi-

lisation Physico-Chimique. Ph.D. Thesis, Ecole nationale supérieure Mines-Télécom Lille Douai.

[31] Siddique, F. (2008) Waste Materials and By-Products in Concrete. Springer Press.

[32] Association Française de Normalisation (AFNOR), XP P13-901 (2001) Blocs de terre comprimée pour murs et cloisons: définitions, spécifications, méthodes d'essai et conditions de réception, Association française de normalisation.

[33] Ayadat, T. and Ouali, S. (1999) Identification des sols affaissables basée sur les limites d'Atterberg. *Revue Française de Géotechnique*, No. 86, 53-56. https://doi.org/10.1051/geotech/1999086053

[34] Levacher, D., Suriray, A., Ndahirwa, D., Zmamou, H., Leblanc, N. and Shimpo, T. (2025) Sediment-Based Unfired Bricks Reinforced with Waste Flax Fibers: Implementation, Physical Aspects and Kinetics of Air Drying—Part I. *Applied Sciences*, **15**, Article 909. https://doi.org/10.3390/app15020909

[35] Glocheux, Y., Pasarín, M.M., Albadarin, A.B., Allen, S.J. and Walker, G.M. (2013) Removal of Arsenic from Groundwater by Adsorption onto an Acidified Laterite By-product. *Chemical Engineering Journal*, **228**, 565-574. https://doi.org/10.1016/j.cej.2013.05.043

[36] Liew, Y., Heah, C., Mohd Mustafa, A.B. and Kamarudin, H. (2016) Structure and Properties of Clay-Based Geopolymer Cements: A Review. *Progress in Materials Science*, **83**, 595-629. https://doi.org/10.1016/j.pmatsci.2016.08.002

[37] Tchadjié, L.N., Djobo, J.N.Y., Ranjbar, N., Tchakouté, H.K., Kenne, B.B.D., Elimbi, A., *et al.* (2016) Potential of Using Granite Waste as Raw Material for Geopolymer Synthesis. *Ceramics International*, **42**, 3046-3055. https://doi.org/10.1016/j.ceramint.2015.10.091

[38] Olaremu, A.G. (2015) Physico-Chemical Characterization of Akoko Mined Kaolin Clay. *Journal of Minerals and Materials Characterization and Engineering*, **3**, 353-361. https://doi.org/10.4236/jmmce.2015.35038

[39] Uchino, T., Sakka, T., Hotta, K. and Iwasaki, M. (1989) Attenuated Toatal Reflectance Fourier-Transform Infrared Spectra of a Hydrated Sodium Soilicate Glass. *Journal of the American Ceramic Society*, **72**, 2173-2175. https://doi.org/10.1111/j.1151-2916.1989.tb06051.x

[40] Criado, M., Fernández-Jiménez, A., Palomo, A., Sobrados, I. and Sanz, J. (2008) Effect of the SiO_2/Na_2O Ratio on the Alkali Activation of Fly Ash. Part II: ^{29}Si MAS-NMR Survey. *Microporous and Mesoporous Materials*, **109**, 525-534. https://doi.org/10.1016/j.micromeso.2007.05.062

[41] Kamwa, R.A.T., Tome, S., Nemaleu, J.G.D., Noumbissie, L.T., Tommes, B., Eguekeng, I., *et al.* (2023) Effect of Curing Temperature on Properties of Compressed Lateritic Earth Bricks Stabilized with Natural Pozzolan-Based Geopolymer Binders Synthesized in Acidic and Alkaline Media. *Arabian Journal for Science and Engineering*, **48**, 16151-16165. https://doi.org/10.1007/s13369-023-08069-0

[42] Kazmi, S.M.S., Munir, M.J., Wu, Y., Hanif, A. and Patnaikuni, I. (2018) Thermal Performance Evaluation of Eco-Friendly Bricks Incorporating Waste Glass Sludge. *Journal of Cleaner Production*, **172**, 1867-1880. https://doi.org/10.1016/j.jclepro.2017.11.255

[43] Kim, J., Yi, C. and Zi, G. (2015) Waste Glass Sludge as a Partial Cement Replacement in Mortar. *Construction and Building Materials*, **75**, 242-246. https://doi.org/10.1016/j.conbuildmat.2014.11.007

[44] Eliche-Quesada, D., Martínez-García, C., Martínez-Cartas, M.L., Cotes-Palomino,

M.T., Pérez-Villarejo, L., Cruz-Pérez, N., *et al.* (2011) The Use of Different Forms of Waste in the Manufacture of Ceramic Bricks. *Applied Clay Science*, **52**, 270-276. https://doi.org/10.1016/j.clay.2011.03.003

[45] Sandra, N. (2024) Influence of Firing Temperature on the Mechanical Properties of Bricks. *International Journal of Geomate*, **26**, 124-131. https://doi.org/10.21660/2024.117.g13381

[46] Zemánek, D., Lang, K., Tvrdík, L., Všianský, D., Nevřivová, L., Štursa, P., *et al.* (2021) Development and Properties of New Mullite Based Refractory Grog. *Materials*, **14**, Article 779. https://doi.org/10.3390/ma14040779

[47] Tchadjie Noumbissie, L. (2012) Comportement Thermique des Géopolymères Obtenus à partir d'une Argile Kaolinite. Master's Thesis, Université de Yaoundé I.

[48] SNI 15-2094-2000 (2000) Indonesia Standard. Massive Red Bricks for Masonry Works. National Standardization Agency of Indonesia.

[49] Omar, M.A.Z.B. (2023) Flexural Strength of Plain Concrete Beam Strengthened with Woven Kenaf FRP Plate: Experimental Works and Numerical Modelling. Ph.D. Thesis, University Tun Hussein Onn (Malaysia).

[50] Bohi, Z.P.B. (2008) Caractérisation des Sols Latéritiques Utilisés en Con-struction Routière: Le Cas de la Région de l'AGNEBY (Cote d'Ivoire). Ph.D. Thesis, École Nationale des ponts et chaussées.

[51] Correa-Jaramillo, R. and Hernández-Olivares, F. (2024) Sustainability in Construction: Geopolymerized Coating Bricks Made with Ceramic Waste. *Materials*, **18**, Article 103. https://doi.org/10.3390/ma18010103

[52] (2003) Masonry Units and Segmental Pavers and Flags-Methods of Test Determining Compressive Strength of Masonry Units. AS/NZS 4456.4, SAI Global Limited.

[53] Hantaniaina, R., Miravo Finarit, R.K., Jean de Dieu, R. and Antoine, A.P. (2023) Contribution a L'Etude des Briques de Terre Comprimées et Stabilisées par le Mélange Chaux—Ciment sur la Satisfaction des Occupants dans les Résidences Modernes Durables Naturellement Ventilées En Zone Tropicale «Cas De L'Ile De Madagascar». *International Journal of Progressive Sciences and Technologies*, **39**, 226-234. https://doi.org/10.52155/ijpsat.v39.1.5396

[54] Fouladi, N., Hamidpour, S., Sedghamiz, M.A. and Rahimpour, M.R. (2021) Application of Biomass Ash for Brick Manufacturing. In: Rahimpour, M.R., *et al.*, Eds., *Advances in Bioenergy and Microfluidic Applications*, Elsevier, 407-429. https://doi.org/10.1016/b978-0-12-821601-9.00017-0

[55] Miraucourt, D. (2017) Stabilisation du Matériau Terre Crue pour Application en Brique de Terre Comprimée au Burkina Faso. Master's Thesis, 2iE—Institut International d'Ingénierie de l'Eau et de l'Environnement.